The Journal of Physical Chemistry A

 VOLUME 101, NUMBER 39, SEPTEMBER 25, 1997

LETTERS

Probe-Wavelength Dependency of Picosecond Anti-Stokes Raman Spectra of *trans*-Stilbene in the S_1 State

Takakazu Nakabayashi,[†] Hiromi Okamoto,*[,†] and Mitsuo Tasumi[‡]

Department of Chemistry and Research Centre for Spectrochemistry, School of Science, The University of Tokyo, Bunkyo-ku, Tokyo 113, Japan, and Department of Chemistry, Faculty of Science, Saitama University, Urawa, Saitama 338, Japan

Received: May 2, 1997; In Final Form: July 2, 1997[⊗]

The picosecond anti-Stokes Raman spectra of *trans*-stilbene in the S_1 state have been observed by using several probe wavelengths (580−670 nm) and a fixed pump wavelength giving a sufficient excess vibrational energy (≈5200 cm^{-1}). The probe-wavelength dependency of the ratio of the anti-Stokes Raman-band intensity at 1180 cm^{-1} due to the C−Ph stretching (ν_{15}) to that at 1570 cm^{-1} due to the olefinic C═C stretching (ν_7) is analyzed by assuming a model based on the Franck−Condon mechanism. It has been shown from the anti-Stokes intensity analysis that vibrationally excited transients at 0 ps delay time are mostly on the lowest excited vibrational levels of the S_1 state as far as the ν_{15} and ν_7 modes are concerned, and the excess energy is not statistically distributed to other modes. A possible mechanism that accounts for this observation is discussed.

Introduction

Vibrational relaxation in polyatomic molecules in solution is an important elementary process in photochemical reactions following photoexcitation. In solution, vibrational relaxation is considered to proceed in several steps.[1] Immediately after photoexcitation, excess vibrational energy is considered to localize in Franck−Condon (FC) active modes. The localized excess energy is first distributed within the molecule to other vibrational modes (intramolecular vibrational redistribution, IVR). Very rapid redistribution of the excess energy creates a quasi-equilibrium among all intramolecular vibrational modes, resulting in a single, mode-independent vibrational temperature. This randomized vibrational energy then dissipates to the surrounding medium (vibrational cooling, VC).

Among various means of time-resolved spectroscopies, time-resolved anti-Stokes Raman spectroscopy allows direct monitoring of vibrational relaxation dynamics, since it probes only the vibrationally excited molecules. Several groups have recently reported transient anti-Stokes Raman spectra of vibrationally hot molecules to obtain information on the IVR and VC processes in solution.[2−11]

Photophysics of *trans*-stilbene is of considerable interest from various viewpoints, for example, in studying the mechanism of the *cis*−*trans* photoisomerization. The dynamics of *trans*-stilbene in the optically allowed lowest excited singlet (S_1) state has been studied extensively by various spectroscopic techniques, including time-resolved (or transient) Raman spectroscopy.[12−14] Recently, two groups have reported the anti-Stokes Raman spectra of S_1 *trans*-stilbene in the high-wavenumber region (up to ≈1600 cm^{-1}).[5,6] Qian et al. have suggested from the analysis of temporal behavior of the anti-Stokes Raman intensities that a nonstatistical distribution of excess energy

* To whom correspondence should be addressed. E-mail: aho@music.email.ne.jp.
[†] The University of Tokyo.
[‡] Saitama University.
[⊗] Abstract published in *Advance ACS Abstracts,* September 15, 1997.

S1089-5639(97)01495-3 CCC: $14.00

persists for several picoseconds.[5] In other words, it takes at least several picoseconds to complete the IVR process. This result is different from the generally accepted view that the time scale of IVR is in the subpicosecond range for large molecules in solution[1] and needs further experimental verification.

To obtain a deeper insight into the IVR process, it is important to know the energy states of the vibrationally excited transients. We have shown that anti-Stokes resonance Raman excitation profiles (REPs) are useful for elucidating the vibrational relaxation process, especially for determining the energy levels on which vibrationally excited transients are populated.[10,11] In the present study, we apply this method to S_1 *trans*-stilbene. We observe the picosecond anti-Stokes Raman spectra of the excited *trans*-stilbene, with a pump wavelength chosen to give the excess vibrational energy greater than 5000 cm^{-1}. Such a large amount of excess energy produces a substantial population on highly excited vibrational levels of FC active high-wavenumber modes. With the pump wavelength fixed, probe-wavelength dependencies of picosecond anti-Stokes Raman intensities are observed and compared with simulated anti-Stokes REPs, to examine the vibrational energy levels of the transients. Whether the excess energy is statistically distributed or not is also analyzed.

Experimental Section

The spectrometer for time-resolved Raman measurements was already described elsewhere.[11] A beam from a frequency-doubled cw mode-locked Nd:YLF laser was used to excite two synchronously-pumped dye lasers, whose outputs were amplified by dye amplifiers. The dye amplifiers were excited by the second harmonic of a cw Nd:YLF regenerative amplifier. The amplified pulses with ≈3 ps duration were obtained at a repetition rate of 1 kHz.

The output from one of the dye amplifiers (554 nm) was frequency-doubled to produce an ultraviolet (277 nm) pump beam. The wavelength of the other amplified dye laser was tuned in the 550−670 nm region and used as a probe beam. The pump and probe beams were collinearly focused on the sample solution (≈0.3 mm thickness liquid jet). The average power of the probe laser was ≈0.2 mW for the Stokes Raman measurement and ≈1 mW for the anti-Stokes Raman measurement. The average power of the pump laser was ≈1 mW for both cases. The spot area was $\approx 1 \times 10^{-3}$ cm^2. The transient signal intensities were found to be proportional to both the pump and probe powers under these conditions.[18] This gives a basis to the intensity analysis described later. Because of the timing jitter between the pump and probe pulses, the cross-correlation time was found to be 5−7 ps,[15] which corresponds to the temporal resolution of this measurement system. The Raman signal was analyzed by a triple polychromator and a CCD detector. The concentration of the sample solution (solvent, 1-butanol) was $1-5 \times 10^{-3}$ mol dm^{-3}.

Results and Discussion

The probe-wavelength dependency of picosecond anti-Stokes Raman spectra of S_1 *trans*-stilbene at 0 ps delay time is shown in Figure 1. We have used eight probe wavelengths, all of which are resonant or pre-resonant with the $S_n \leftarrow S_1$ electronic absorption around 585 nm.[12] The Stokes Raman spectrum at a delay time of 30 ps is also shown in this figure (probe wavelength, 590 nm). The pump wavelength 277 nm corresponds to an energy ≈5200 cm^{-1} above the origin of the $S_1 \leftarrow S_0$ absorption (the 0−0 band) at ≈30 890 cm^{-1}. In Figure 1, three strong features are observed, all of which are attributed to S_1 *trans*-stilbene.[16,17] The relatively broad Raman band at

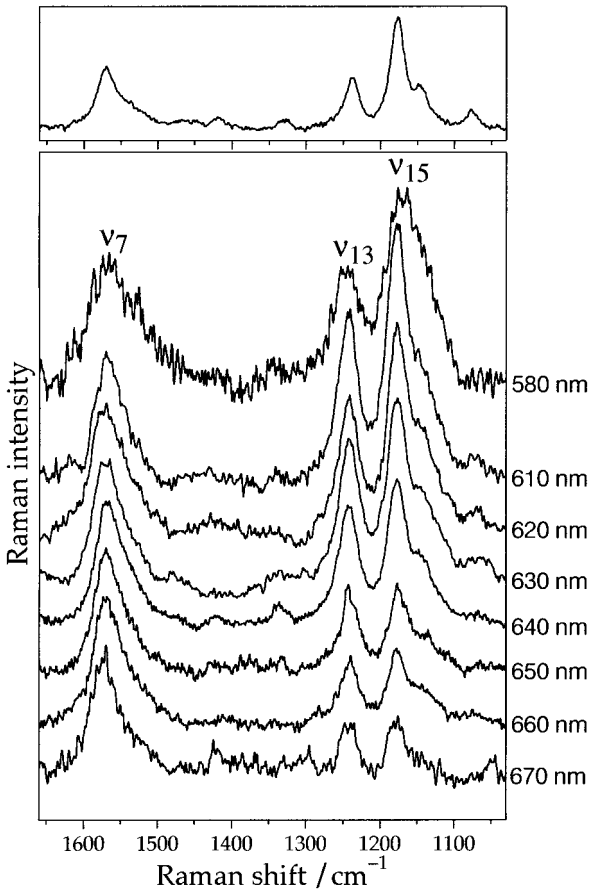

Figure 1. (top) Stokes Raman spectrum of *trans*-stilbene in the S_1 state at 30 ps after photoexcitation in a 1-butanol solution. The Raman bands of the solvent are subtracted; pump, 277 nm; probe, 590 nm. (bottom) Anti-Stokes Raman spectra of *trans*-stilbene in the S_1 state at 0 ps after photoexcitation in a 1-butanol solution. Pump, 277 nm; probe, given on the right of each spectrum. Each spectrum is normalized by using the intensity of the olefinic C═C stretching (ν_7) band at 1570 cm^{-1} as a reference.

≈1570 cm^{-1} is assigned to ν_7, the olefinic C═C stretch, and the band at ≈1240 cm^{-1} to ν_{13}, the olefinic C−H in-plane bend. Another band at ≈1180 cm^{-1} is due to ν_{15}, a mode with a major contribution from the C−Ph stretch.[16,17]

Generally speaking, anti-Stokes Raman intensities for high-wavenumber modes are weak, because of small populations on their vibrationally excited states. In Figure 1, on the contrary, the anti-Stokes Raman intensity of the ν_7 band is comparable to, or even stronger than, those of the ν_{13} and ν_{15} bands. The intensity of the ν_{15} band relative to that of the ν_7 band shows a maximum at 610 nm probe and decreases markedly as the probe wavelength becomes longer. Two different factors should be considered to explain this observation. One is concerned with vibrationally excited populations. Since the excess vibrational energy is ≈5200 cm^{-1} immediately after photoexcitation, it is likely that a FC active high-wavenumber mode like ν_7 is highly excited. The other factor is related to REPs of the anti-Stokes scattering. In general, the anti-Stokes intensity of a higher-wavenumber mode shows a maximum in the REP in the excitation-wavelength region longer than that of a lower-wavenumber mode.[10] A quantitative analysis of the anti-Stokes REPs is important for determining the energy levels of vibrationally excited transients. Thus, anti-Stokes REPs are calculated for various vibrationally excited (initial) levels and compared with the observed results.

The method of simulation was the same as that adopted in the case of a carotenoid.[10,11] It was based on the A-term of

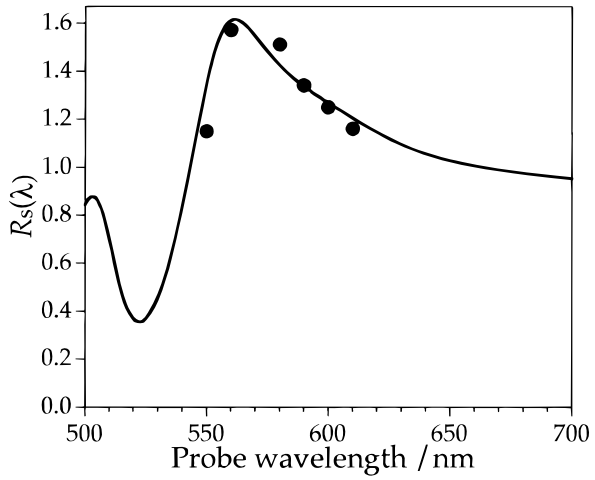

Figure 2. Probe-wavelength dependency of the Stokes Raman intensity ratio $R_s(\lambda)$. Solid curve, simulated; filled circles, observed at 30 ps delay time.

Albrecht's formula (FC mechanism). The $S_n \leftarrow S_1$ absorption spectrum was also simulated on the basis of the FC mechanism.[18] In the simulation, only three strongly Raman active vibrational modes, ν_7, ν_{13}, and ν_{15}, were considered. In the harmonic approximation and in the absence of the Duschinsky rotation and changes in vibrational frequencies on going from the S_1 to S_n state, the FC factor in the Raman tensor can be given as an analytical function of potential displacements (Δ_i's) between the S_1 and S_n states, along the (dimensionless) normal coordinates of ν_i's. We adjusted Δ_i's, Γ_H (homogeneous half-width), ν_{IH} (inhomogeneous half-width), and E_0 (0−0 energy separation for the $S_n \leftarrow S_1$ transition) to obtain good fits between the observed and simulated results.

Molecules giving rise to Stokes Raman scattering at 30 ps delay time are mostly on the $n = 0$ level for high-wavenumber modes (i.e., the observed transition corresponds to $1 \leftarrow 0$). Thus, we first simulated the $1 \leftarrow 0$ Stokes REPs to check the validity of the theoretical model. For determining the Raman intensities of the photoexcited transient, solvent Raman bands are not adequate as the intensity reference, because the concentration of the transient may be seriously affected by fluctuation of the pump-pulse energy. Hence, the fitting procedure was performed on the relative Raman intensity of two bands attributed to the S_1 species. Figure 2 shows the simulated probe-wavelength dependency of the ratio of the Stokes intensity of the ν_{15} band to that of the ν_7 band [$R_s(\lambda) \equiv I_{15}(\lambda)/I_7(\lambda)$, where $I_{15}(\lambda)$ and $I_7(\lambda)$ denote, respectively, the ν_{15} and ν_7 Raman intensities at excitation (probe) wavelength λ], together with the observed data. The parameters used for the simulation were $\Delta_7 = 0.43$, $\Delta_{13} = 0.35$, $\Delta_{15} = 0.51$, $\Gamma_H = 380\ cm^{-1}$, $\nu_{IH} = 420\ cm^{-1}$ and $E_0 = 17\,185\ cm^{-1}$. The agreement between the observed and simulated curves is satisfactory. A similar intensity ratio for the ν_{13} Stokes band [$I_{13}(\lambda)/I_7(\lambda)$] and the $S_n \leftarrow S_1$ absorption spectrum were also well reproduced by the same parameter set.[18]

Actually, the observed $R_s(\lambda)$ was reproduced even more satisfactorily by calculation using only a homogeneous broadening function ($\Gamma_H = 600\ cm^{-1}$) and slightly changed Δ values ($\Delta_7 = 0.43 \rightarrow 0.42$, $\Delta_{13} = 0.35$, $\Delta_{15} = 0.51 \rightarrow 0.52$), without using an inhomogeneous broadening function. Thus, it seems to be infeasible to determine reliable values for the broadening parameters from the observed results, but it is clear that the mathematical model of the vibronic band shape has little effect on the following discussion.

The results mentioned above for the Stokes profiles and the transient absorption give a solid basis to the following analysis

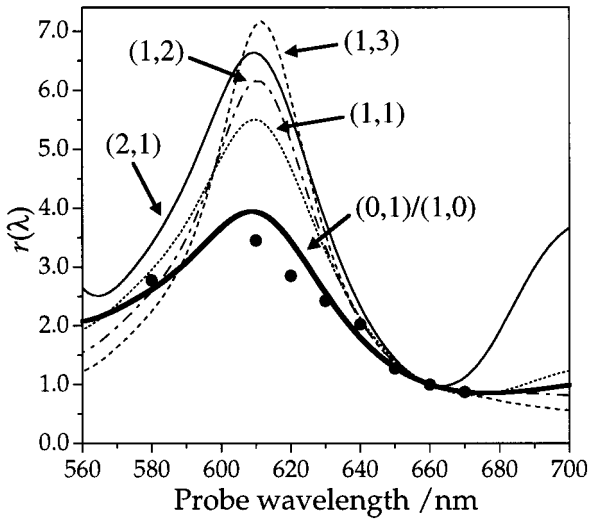

Figure 3. Probe-wavelength dependency of the normalized anti-Stokes Raman intensity ratio $r(\lambda)$ for $\lambda_0 = 660$ nm. Filled circles, observed points at 0 ps delay time; curves (n_7, n_{15}), simulated for the initial states with quantum numbers n_7 and n_{15} for the ν_7 and ν_{15} vibrational modes, respectively; curve (0,1)/(1,0), simulated for the ν_{15} and ν_7 bands due to the (0,1) → (0,0) and (1,0) → (0,0) transitions, respectively.

of anti-Stokes profiles. The analysis of the anti-Stokes REPs are performed on the relative Raman intensity of two bands for the same reason as described for the Stokes REPs. The ratio of the observed anti-Stokes intensity of the ν_{15} band to that of the ν_7 band at λ, $R_{as}(\lambda)$, is given by

$$R_{as}(\lambda) \equiv \frac{I_{15}(\lambda)}{I_7(\lambda)} = \frac{P_{15} I_{15}'(\lambda)}{P_7 I_7'(\lambda)} \qquad (1)$$

where $I_7'(\lambda)$ and $I_{15}'(\lambda)$ are the simulated anti-Stokes Raman intensities and P_7 and P_{15} represent the populations on the initial (vibrationally excited) levels, which are not considered in simulating the Stokes REPs. It is clear from this equation that the observed $I_{15}(\lambda)/I_7(\lambda)$ cannot be directly compared with the simulated $I_{15}'(\lambda)/I_7'(\lambda)$, unless P_{15}/P_7 is known. However, it is possible to remove P_{15}/P_7 by taking the following ratio, $r(\lambda)$, which will be called the normalized intensity ratio

$$r(\lambda) \equiv \frac{R_{as}(\lambda)}{R_{as}(\lambda_0)} = \frac{I_{15}(\lambda)\, I_7(\lambda_0)}{I_7(\lambda)\, I_{15}(\lambda_0)} = \frac{I_{15}'(\lambda)\, I_7'(\lambda_0)}{I_7'(\lambda)\, I_{15}'(\lambda_0)} \qquad (2)$$

where λ_0 is an arbitrary wavelength chosen for a reference. Then, a direct comparison between the simulated and observed $r(\lambda)$ values may be made.

In Figure 3, $r(\lambda)$'s for $\lambda_0 = 660$ nm simulated for several initial levels are shown. In the cases treated in this figure, the energies of the initial levels are below the energy of the pump pulse, i.e., 5200 cm^{-1} above the 0−0 band of the $S_1 \leftarrow S_0$ transition. The parameters used for the simulation are the same as those for Figure 2. The observed $r(\lambda)$ at 0 ps delay time is also shown in this figure. All the observed points are corrected for the ν^4 factor. Dependence of detection sensitivity against wavelength was found to be negligibly small in this wavelength region. The linearities of the Raman intensities against the pump power indicate that effects of reabsorption of the scattered light by the transient species would be insignificant. We assume that the ν_7 and ν_{15} anti-Stokes Raman bands arise from a common excited level [(1,1), (1,2), (1,3), or (2,1), where n_7 and n_{15} of (n_7, n_{15}) represent the vibrational quantum numbers of the ν_7 and ν_{15} modes, respectively] or from the lowest excited levels [(1,0) for the ν_7 band and (0,1) for the ν_{15} band]. If the

vibrational excitation is extremely localized on the ν_7 mode, for example, this assumption is not correct. In the present case, the pump-wavelength dependency of the picosecond anti-Stokes Raman spectra indicates that both ν_7 and ν_{15} modes are substantially excited at 0 ps delay time, when pump photons with a sufficiently high excess energy are used.[18] Hence, the above consideration may be rationalized.

All the simulated curves in Figure 3 show maxima at ≈610 nm, in agreement with the experimental observation. However, each curve has a shape and a maximum value of $r(\lambda)$ different from others. Such features can be utilized for the determination of the initial state involved. Clearly, the observed points are best reproduced by the (0,1)/(1,0) curve, which is calculated on the assumption that both the ν_7 and ν_{15} bands arise from the lowest excited vibrational levels. This result leads us to a conclusion that the vibrationally excited transients at 0 ps delay time are mostly on the lowest excited vibrational levels of the S_1 state, as far as the ν_7 and ν_{15} modes are concerned.

The S_1 *trans*-stilbene gives another strong low-wavenumber Raman band at 285 cm^{-1}, which is assigned to the C_o-C-C bend (ν_{24}, C_o represents the ethylenic carbon). With our present spectrograph, however, we cannot obtain reliable experimental results for this band to estimate the Δ_{24} value, because of interference by emission from the dye amplifier. This mode might have some effects on the excitation profiles, and an examination of those effects under various conditions is now underway.[18] Preliminary results show that the inclusion of the ν_{24} mode lowers the maximum values of $r(\lambda)$. However, changes in $r(\lambda)$ are no more than ≈10% unless vibrational populations on the $n \geq 1$ levels of this mode are exceptionally large, even if Δ_{24} is as large as 0.51 (the same value as Δ_{15}). To populate the $n \geq 1$ levels of the ν_{24} mode, the displacement between the equilibrium geometries of the S_0 and S_1 states along this mode must be large. Since no strong band assignable to the ν_{24} mode seems to be observed in the Raman spectrum of S_0 *trans*-stilbene in resonance with the $S_1 \leftarrow S_0$ transition,[19] the displacement along the ν_{24} mode must be small. It is then unlikely that this mode is highly excited on the $S_1 \leftarrow S_0$ photoexcitation. This means that the $n \geq 1$ populations for this mode are not large. Hence, the calculated (0,1)/(1,0) curve in Figure 3 would not change greatly even if the contribution of the ν_{24} mode is considered. The Δ values for the other vibrational modes are smaller than the values of Δ_7, Δ_{13}, and Δ_{15} used in the present simulation, and they have only minor effects on $r(\lambda)$.

What should be discussed next, on the basis of the above conclusion, is whether the molecules giving rise to the transient anti-Stokes scattering are in intramolecular thermal equilibria or not. The question may be rephrased as follows: Is the IVR process completed within our temporal resolution (5−7 ps), or is the excess energy still localized on a few modes in the same time range ? To examine this point, we simulate the $R_{as}(\lambda)$ of a case where the excess energy is thermally distributed and compare it with the observed value at 0 ps delay time.

In a thermal equilibrium, the factor P_{15}/P_7 in eq 1 corresponds to the ratio of Boltzmann factors for the initial levels. To estimate the Boltzmann factors, we need to know the intramolecular vibrational temperature after the absorption of the pump energy. This can be found by assuming that the whole excess energy (≈5200 cm^{-1}) is distributed among all intramolecular vibrational modes according to the Boltzmann distribution. Since the vibrational wavenumbers of the S_1 species are known only for a few modes, we introduce an approximation that the vibrational modes of S_1 *trans*-stilbene (72 in total) lie at equal intervals between 0 and 1600 cm^{-1}, except for the C−H stretches (12 modes), which are assumed to have a single wavenumber of 3000 cm^{-1}. The intramolecular vibrational temperature thus calculated is ≈550 K. This value of calculated temperature changes when a different set of intramolecular vibrational wavenumbers is adopted. Uncertainty of the calculated temperature is estimated to be ≈±50 K from several trials with different vibrational wavenumber sets. The simulated $R_{as}(\lambda)$ for a thermal equilibrium at a solute temperature of 550 K is shown in Figure 4, together with the observed $R_{as}(\lambda)$ at 0 ps delay time. In Figure 4, the simulated $R_{as}(\lambda)$ curve has substantially larger values than the observed ones. To explain the observed $R_{as}(\lambda)$ based on the statistical distribution, the solute temperature must be assumed to be much higher than 1000 K, which is clearly outside the uncertainty range for the calculated temperature. The large discrepancy between the calculated and observed results clearly shows that the anti-Stokes scattering obtained at 0 ps delay time arises from molecules in which excess energy is not statistically distributed. In view of the temporal resolution of the present experiment, it may be concluded that it takes several picoseconds or longer to reach an intramolecular thermal equilibrium in S_1 *trans*-stilbene.

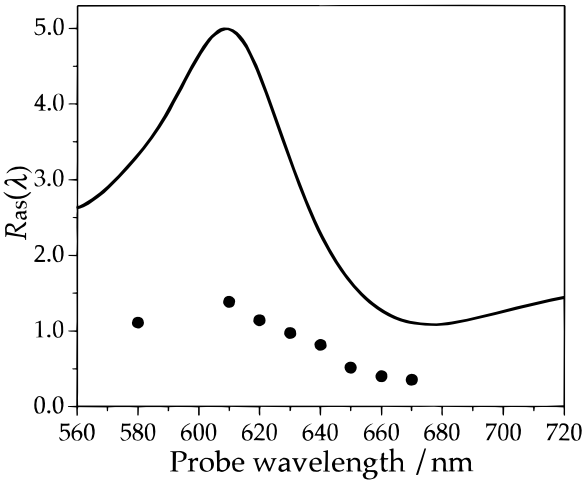

Figure 4. Probe-wavelength dependency of the anti-Stokes Raman intensity ratio $R_{as}(\lambda)$. Solid curve, simulated for a thermal equilibrium at 550 K; filled circles, observed at 0 ps delay time.

Our conclusion seems to be consistent with the work of Qian et al., which suggests that the IVR time of S_1 *trans*-stilbene in solution is >3−5 ps, from the temporal behavior of the anti-Stokes intensities.[5] In addition, we have further obtained an important result on the IVR dynamics that the anti-Stokes bands (at 0 ps delay time) due to the olefinic modes, namely, the olefinic C═C stretching and C−Ph stretching modes, arise mostly from their lowest excited vibrational levels of the S_1 state, although a pump light with a large amount of excess vibrational energy (≈5200 cm^{-1}) is used.

The above conclusion suggests that the intramolecular vibrational relaxation process of S_1 *trans*-stilbene proceeds in roughly two steps. The molecule may be highly excited for the FC active high-wavenumber modes immediately after photoexcitation, and it relaxes very rapidly (probably in the femto- to subpicosecond time range) to the lowest vibrationally excited levels of the S_1 state. Then, slower relaxation (in several picoseconds) occurs to achieve an intramolecular thermal equilibrium. The VC process may follow after that. This means that, even in a large molecule such as *trans*-stilbene, there is a bottleneck state in the intramolecular vibrational relaxation in solution.[20]

References and Notes

(1) Elsaesser, T.; Kaiser, W. *Annu. Rev. Phys. Chem.* **1991**, *42*, 83.
(2) Hayashi, H.; Brack, T. L.; Noguchi, T.; Tasumi, M.; Atkinson, G. H. *J. Phys. Chem.* **1991**, *95*, 6797.
(3) Phillips, D. L.; Rodier, J.-M.; Myers, A. M. *Chem. Phys.* **1993**, *175*, 1.
(4) Sato, S.; Kitagawa, T. *Appl. Phys. B* **1994**, *59*, 415.
(5) Qian, J.; Schultz, S. L.; Jean, J. M. *Chem. Phys. Lett.* **1995**, *233*, 9.
(6) Matousek, P.; Parker, A. W.; Toner, W. T.; Towrie, M.; de Faria, D. L. A.; Hester, R. E.; Moore, J. N. *Chem. Phys. Lett.* **1995**, *237*, 373.
(7) Shreve, A. P.; Mathies, R. A. *J. Phys. Chem.* **1995**, *99*, 7285.
(8) Nakabayashi, T.; Okamoto, H.; Tasumi, M. *J. Raman Spectrosc.* **1995**, *26*, 841.
(9) Huang, Y.; Hopkins, J. B. *J. Phys. Chem.* **1996**, *100*, 9585.
(10) Okamoto, H.; Nakabayashi, T.; Tasumi, M. *J. Phys. Chem. A* **1997**, *101*, 3488.
(11) Nakabayashi, T.; Okamoto, H.; Tasumi, M. *J. Phys. Chem. A* **1997**, *101*, 3494.
(12) Hochstrasser, R. M. *Pure Appl. Chem.* **1981**, *52*, 2683.
(13) Waldeck, D. H. *Chem. Rev. (Washington, D.C.)* **1991**, *91*, 415.
(14) Hamaguchi, H.; Gustafson, T. L. *Annu. Rev. Phys. Chem.* **1994**, *45*, 593.
(15) Okamoto, H.; Tasumi, M. *Rev. Sci. Instrum.* **1995**, *66*, 5165.
(16) Hamaguchi, H. In *Vibrational Spectra and Structure*; Durig, J. R., Ed.; Elsevier: Amsterdam, 1987; Vol. 16, pp 227−309.
(17) Urano, T.; Hamaguchi, H.; Tasumi, M.; Yamanouchi, K.; Tsuchiya, S.; Gustafson, T. L. *J. Chem. Phys.* **1989**, *91*, 3884.
(18) Nakabayashi, T.; Okamoto, H.; Tasumi, M. Manuscript in preparation.
(19) Myers, A. B.; Trulson, M. O.; Mathies, R. A. *J. Chem. Phys.* **1985**, *83*, 5000.
(20) Owrutsky, J. C.; Raftery, D.; Hochstrasser, R. M. *Annu. Rev. Phys. Chem.* **1994**, *45*, 519.